Brief communication: Uncertainties in Southern Ocean sea surface conditions and their impact on Antarctic climate over 1958–1978

Quentin Dalaiden[1] and Ingo Bethke[2]

[1]Nansen Environmental and Remote Sensing Center and Bjerknes Centre for Climate Research, Bergen, Norway
[2]Geophysical Institute, Bjerknes Centre for Climate Research, University of Bergen, Bergen, Norway

Correspondence: Quentin Dalaiden (quentin.dalaiden@nersc.no)

Abstract. Atmospheric reanalyses extending before 1979, including ERA5, show a substantial cold bias over Antarctica during 1958–1978. Because Southern Ocean sea surface conditions (SSCs) are poorly constrained in this period, we assess their role using two ensembles of a global atmospheric model forced by different SSC datasets. The first uses the widely employed HadISST product, while the second is based on a recent reconstruction that assimilates continental observations. Our results show that SSC differences strongly alter the Antarctic surface climate, but explain only about 30% of the ERA5 cold bias ERA5, indicating that additional factors contribute to this bias.

1 Introduction

Being the largest freshwater reservoir on Earth, any change in the total ice mass of the Antarctic Ice Sheet (AIS) has profound global implications (Fyke et al., 2018), including contributions to sea-level rise affecting coastal regions and impacts on the overturning circulation of the global ocean through the deep-water formation. The total mass balance of an ice sheet is defined as the difference between the surface mass gain, referred to as the surface mass balance (SMB) and dominated by snowfall (e.g., Lenaerts et al., 2020), and the mass losses due to ice-shelf melting and iceberg calving (Fyke et al., 2018). Over 1992–2020, the AIS experienced a net negative mass balance, with ice losses – primarily from ice-shelf melting – exceeding the surface mass gain (Otosaka et al., 2023). However, more recently, during 2020–2023, the AIS showed a slight mass gain (Wang et al., 2025), largely attributed to increased snow accumulation in East Antarctica, while West Antarctica – particularly glaciers located in the Amundsen Sea – has continued to lose mass at a pace comparable to the 1990s. Climate model simulations have long suggested that snowfall over Antarctica should increase in response to atmospheric warming (e.g., Frieler et al., 2015), yet observations until 2020 had not confirmed this model signal. The recent mass gain therefore suggests that snowfall variability may at times be large enough to offset, at least partially, the losses from ice-shelf melting.

The Antarctic SMB is largely controlled by the transport of humidity from the low- and mid-latitude regions of the Southern Hemisphere (e.g., Lenaerts et al., 2020). Sea surface conditions (SSCs) – sea surface temperature and sea-ice concentration – in the Southern Ocean play a substantial role in regulating this moisture transport and, consequently, the variability of Antarctic SMB through air-sea interactions (e.g., Kittel et al., 2018). An ice-free ocean surface enhances air–sea exchanges, increasing the humidity content of the overlying atmosphere, which can subsequently be converted into snowfall over Antarctica during

25 adiabatic cooling associated with orographic uplift. Similarly, warmer seas act to increase humidity transport to the continent. Since 1979, the year-to-year variability of SSCs has been well constrained thanks to satellite observations, but prior to 1979 large uncertainties remain (e.g., Titchner and Rayner, 2014; Dalaiden et al., 2025). The latest atmospheric reanalyses from the European Centre for Medium-Range Weather Forecasts, ERA5 (Hersbach et al., 2020) – considered as the best state-of-the-art atmospheric reanalyses in Antarctica (e.g., Gossart et al., 2019) –, which extends back to 1940, are therefore sensitive to these

30 uncertainties. Bromwich et al. (2024) identified a pronounced cold bias in ERA5 over Antarctica during the pre-satellite era, particularly 1958–1978, when numerous weather stations became available due to the International Geophysical Year. This bias corresponds to an overestimated warming trend since 1958. Furthermore, polar-oriented regional climate models driven by ERA5 suggest a large SMB increase over this period (van Dalum et al., 2025), raising questions about the reliability of such results given the uncertainties in Southern Ocean SSCs.

35 In this study, we investigate how uncertainties in Southern Ocean SSCs influenced the Antarctic surface climate and large-scale atmospheric circulation during the pre-satellite period (1958–1978). To this end, we use a recently published reconstruction constrained by weather station observations from both Antarctica and mid-latitude regions of the Southern Hemisphere (Dalaiden et al., 2025). To assess the role of SSC uncertainty, we conduct ensembles of global atmospheric circulation model simulations using this reconstruction and, for comparison, the HadISST2 dataset (Titchner and Rayner, 2014), which is used

40 in ERA5. In addition, we evaluate Antarctic climate in ERA5 during 1958–1978, with a particular focus on the extent to which SSCs contribute to the cold bias reported by Bromwich et al. (2024).

2 Data and methods

2.1 Historical Southern Ocean Sea Surface Conditions

To test the sensitivity of the Antarctic surface climate to uncertainties in Southern Ocean SSCs during the 1958–1979 period,

45 we use two different SSC datasets. The first dataset is taken directly from ERA5. This blended product combines HadISST2 (Titchner and Rayner, 2014) prior to 1979 with ERA5 reanalysis fields (Hersbach et al., 2020); after 1979, SSCs are derived from the Operational Sea Surface Temperature and Sea Ice Analysis (OSTIA) product (Good et al., 2020). We use ERA5 SSCs because ERA5 has consistently been shown to provide the most reliable performance among atmospheric reanalyses over Antarctica (e.g., Gossart et al., 2019). However, it is important to note that HadISST2 is known to display a large sea-ice

50 extent (e.g., Titchner and Rayner, 2014). For simplicity, we refer to this blended dataset as "ERA5 SSCs" throughout the text.

The second dataset is the recently published reconstruction of Dalaiden et al. (2025) (hereafter we use the acronym ANT-REC throughout the text), which covers the entire 1958–2023 period for the Southern Ocean. This product combines annual weather station observations – specifically near-surface air temperature and atmospheric surface pressure – from Antarctica and mid-latitudes with ten different Earth System Model ensemble simulations, using a data assimilation framework, resulting

55 in a fully physically consistent atmospheric reanalysis. This atmospheric reanalysis was then used to force an ocean–sea-ice model, thereby reconstructing oceanic variability including sea ice. A key advantage of this dataset is that, unlike ERA5, it is

directly constrained by Antarctic and mid-latitude observations and is not dependent on HadISST2, making it potentially better suited to capture pre-satellite variability.

2.2 Weather stations observations

To evaluate the impacts of SSCs on the Antarctic surface climate, we use long-term instrumental observations from Antarctic weather stations operating since the International Geophysical Year (1958). These records are compiled in the SCAR READER dataset (Turner, 2004). In total, 15 stations provide near-surface air temperature measurements with continuous coverage beginning around 1958. It is important to note that these long-term observations were also used in the reconstruction of Dalaiden et al. (2025). We restrict our analysis to only time-continuous stations in order to avoid artifacts associated with temporal changes in station availability.

2.3 The Community Atmospheric Model (CAM)

To quantify the impact of Southern Ocean SSCs on the Antarctic surface climate during 1958–1978, we use a global atmospheric model with prescribed SSCs (monthly mean sea surface temperature and sea-ice concentration fields). Specifically, we employ the atmospheric component of the Norwegian Earth System Model Version 1 at medium resolution (NorESM1-ME) (Bentsen et al., 2013), namely the Community Atmospheric Model version 4 (CAM4) (Neale et al., 2010), which is based on the Community Earth System Model Version 1 (CESM1) (Hurrell et al., 2013). In this configuration, CAM4 includes a prognostic formulation of the aerosol life cycle, replacing the original prescribed formulation. The model is run on the standard horizontal f19 grid (nominal 2° resolution; 1.9° × 2.5° latitude–longitude) and uses 26 hybrid-sigma vertical levels. Although CAM4 is an older-generation model, Dalaiden et al. (2025) demonstrated that it performs satisfactorily over the Southern Ocean. In addition, external forcings are updated to those used in CMIP5. A further advantage of using CAM4 over newer versions is the computational efficiency, which makes it well suited for ensemble-based experiments at modest computational cost.

2.4 Experiments

The experiments conducted with CAM4 follow the framework of Atmospheric Model Intercomparison Project (AMIP)-style simulations (Gates et al., 1999), in which SSCs are prescribed to isolate their effects on atmospheric variables, including atmospheric circulation. We perform two ensembles of experiments. In the first ensemble, SSCs are taken from ERA5, while in the second they are taken from ANT-REC. The difference between the two ensembles therefore isolates the influence of SSC uncertainties on the Antarctic climate system. Each ensemble consists of ten simulations, all using the same SSCs and external forcings but initialized with small atmospheric perturbations following Kay et al. (2015) (micro-perturbation). The ensembles span the 1959–2000 period. We analyze the ensemble mean in order to amplify the signal from prescribed SSCs and reduce the contribution of internal atmospheric variability.

3 Results

3.1 Historical changes in Southern Ocean sea surface conditions since 1958

Since 1958, substantial changes in both annual mean sea-ice cover and sea surface temperature (SST) have been observed
in the Southern Ocean. Focusing first on sea ice, the total sea-ice extent (defined as the integrated ocean area covered by at
least 15% ice concentration) exhibits pronounced multi-decadal variability that can be broadly divided into three periods (Fig.
1). From 1958 to 1980, an overall decline in sea-ice extent is noticed in both ERA5 and ANT-REC, including a sharp drop
toward the end of this period. This is followed by a relatively steady increase that lasts until 2015, after which another marked
decline is noticed. From 1979 onward, when satellite observations are available, both ERA5 and ANT-REC datasets show good
agreement, although, as noted by Dalaiden et al. (2025), ANT-REC underestimates the 2014 maximum. In contrast, during the
earlier 1958–1978 period, substantial discrepancies emerge: ERA5 exhibits a much larger decrease in sea-ice extent compared
to ANT-REC. Specifically, the change in sea-ice extent between 1981–2000 and 1959–1968 reaches -1.94×10^6 km^2 (-15.4%)
in ERA5, compared to only -0.58×10^6 km^2 (-4.6%) in ANT-REC – nearly three times smaller.
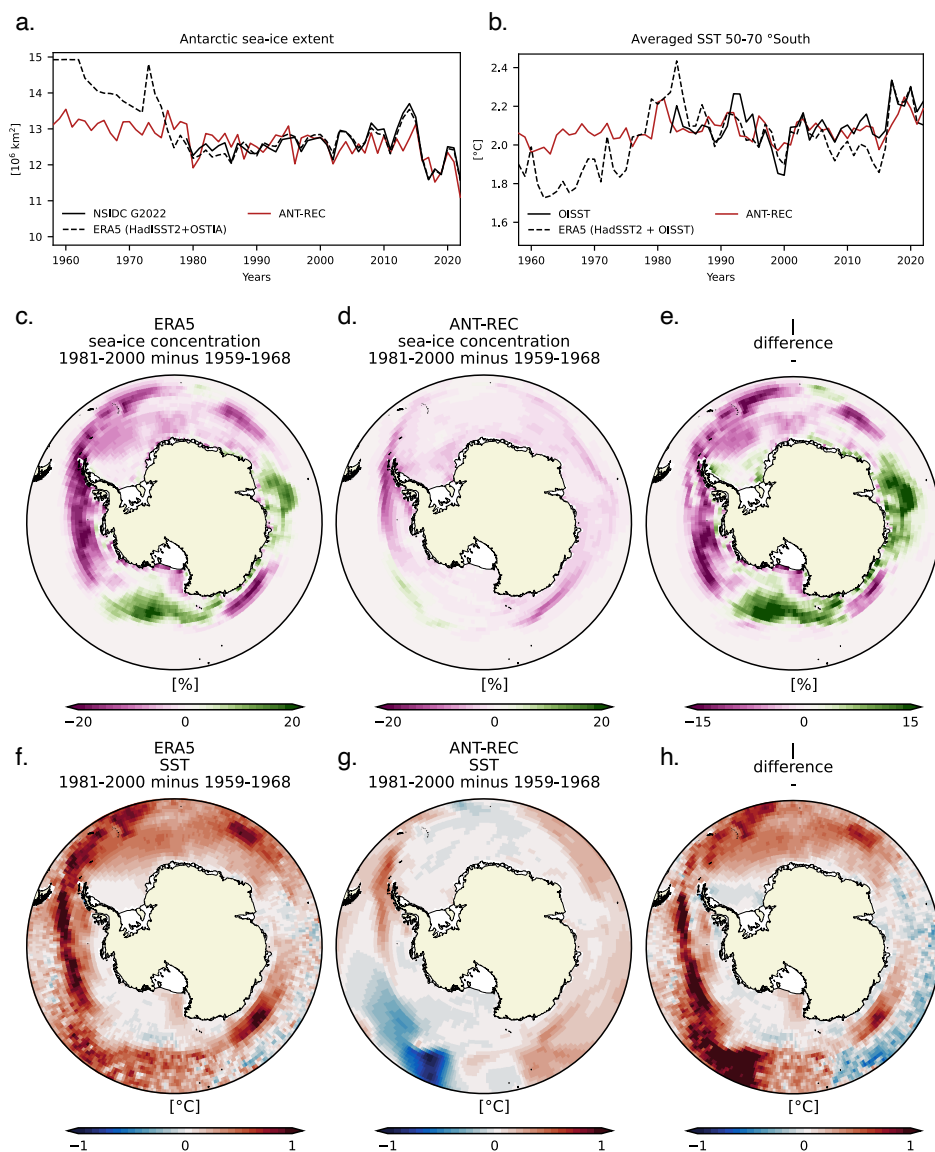
Figure 1. (**a**) Evolution of total annual Antarctic sea-ice extent from 1958 to 2022 in satellite-based observations (NSIDC), ERA5 SSCs, and ANT-REC. (**b**) Southern Ocean mean SST (50–70°S) from OISST, ERA5 SSCs, and ANT-REC. (**c–e**) Sea-ice concentration changes between 1981–2000 and 1959–1968 in ERA5 SSCs (**c**), ANT-REC (**d**), and their difference (**e**). (**f–h**) SST changes between 1981–2000 and 1959–1968 in ERA5 SSCs (**f**), ANT-REC (**g**), and their difference (**h**).

Spatially, ANT-REC suggests relatively uniform changes in sea-ice concentration over 1981–2000 relative to 1959–1968 (we focus on the first 10 years as the differences are the largest), with the largest negative anomalies in the Bellingshausen Sea and a slight increase offshore of the Ross Sea. In contrast, ERA5 (using boundary conditions from HadISST2) reveals both a stronger magnitude of change and larger spatial variability. The most significant declines occur in the Amundsen and Bellingshausen

Seas and in the Atlantic sector, while increases are evident in the Ross Sea and near the Amery Ice Shelf. As a result, the difference between the two datasets highlights a stronger sea-ice decline in ERA5 in the Amundsen and Bellingshausen Seas
105 and the Atlantic sector, whereas in the Indian sector and Ross Sea, ANT-REC indicates a more substantial decrease.

Changes in SSTs are broadly consistent with those in sea-ice extent. The temporal evolution of SSTs averaged over the Southern Ocean (50–70°S) shows colder conditions during 1958–1967 compared to 1981–2010, with a mean difference of -0.28°C in ERA5 and -0.06°C in ANT-REC. Consistent with its underestimation of the 2014 sea-ice maximum, ANT-REC also exhibits a warm SST bias in that year. In terms of spatial patterns, ERA5 indicates relatively homogeneous surface warming
110 across the Southern Ocean, with the strongest anomalies in regions of largest sea-ice loss, as well as farther north – particularly in the Atlantic and Pacific sectors. In contrast, ANT-REC shows greater spatial heterogeneity and a weaker overall warming signal. The strongest SST increases in ANT-REC occur near the Antarctic Peninsula, with moderate warming in the Indian sector, while little to no change is noticed in the Weddell, Ross, and Amundsen Seas. Consequently, ERA5 depicts significantly cooler conditions across the Southern Ocean during 1958–1967 compared to ANT-REC, especially in the Atlantic and
115 Pacific sectors. These discrepancies highlight the 1958–1978 period as a key window of uncertainty in SSC reconstructions, underscoring the importance of quantifying how such differences impact the Antarctic climate over that period.

3.2 Station-based evaluation of near-surface air temperature biases under different SSCs

Fig. 2 shows the bias in annual near-surface air temperature during 1959–1968 for ERA5, ERA5-forced CAM and ANT-REC-forced CAM, relative to weather station observations. Before computing the bias (defined as the difference between each dataset
120 and station observations), all datasets were first expressed as anomalies with respect to the 1981–2000 mean. In addition, for both the ERA5-forced and ANT-REC-forced CAM ensembles, 1,000 bootstrap resamples were generated from the 10-member ensemble to quantify the contribution of internal atmospheric variability to the total signal. ERA5 exhibits a cold bias at most stations (-0.68°C on average). In ERA5-forced CAM, the cold bias persists but is weaker (-0.38°C). This indicates that although the continental cold bias in ERA5 is partly related to the prescribed SSCs, SSCs alone cannot fully account for it. In
125 ANT-REC-forced CAM, the mean temperature bias is slightly negative (0.04 °C). The positive temperature bias contrasts with ERA5-forced CAM and is consistent with the smaller sea-ice extent and warmer SSTs in ANT-REC compared to ERA5 SSCs.
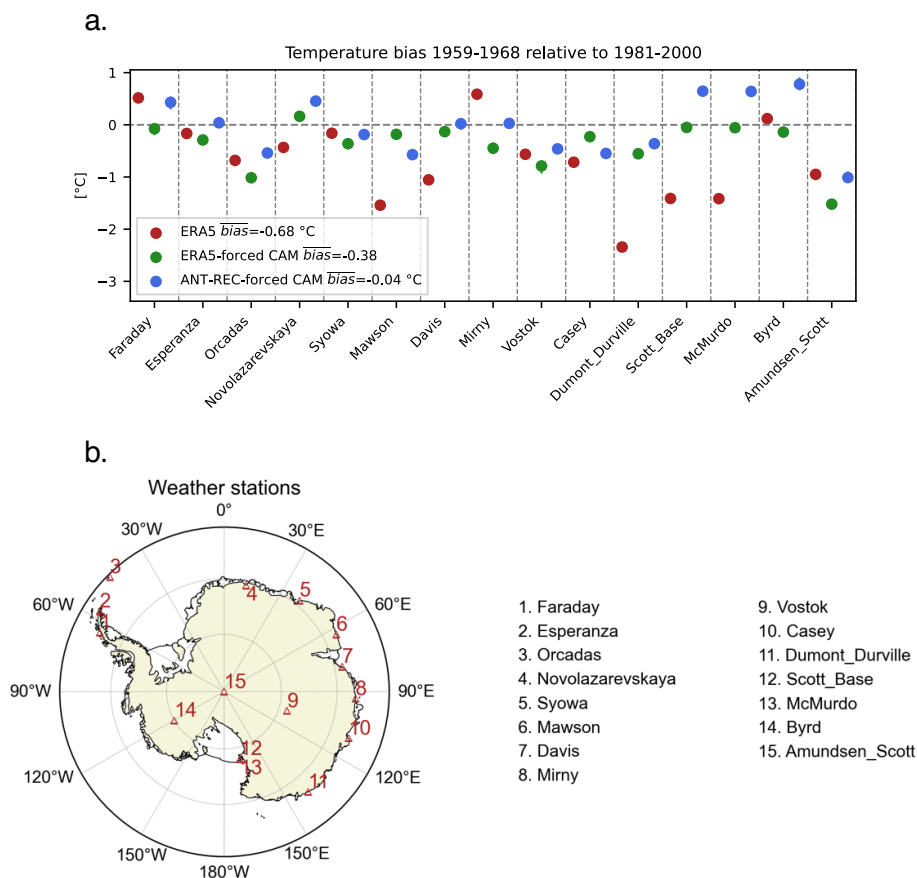
Figure 2. (**a**) Bias in annual near-surface air temperature relative to weather station observations over 1959–1968 for ERA5 , ERA5-forced CAM and ANT-REC-forced CAM. The bias is defined as model or reanalysis minus observations (e.g., negative values indicate a cold bias). All time series are expressed as anomalies relative to the 1981–2000 mean before bias calculation. For the two CAM ensembles, the dots indicate the median of the 1,000 bootstrap resamples derived from the 10-member ensemble, while the bars represent the 95% confidence interval. (**b**) Locations of the weather stations.

3.3 Changes in precipitation and near-surface air temperature over the Antarctic Ice Sheet associated with sea surface condition changes

Fig. 3 shows the changes in precipitation and near-surface temperature between 1959–1968 and 1981–2000 from the CAM
130 ensemble mean using ANT-REC SSCs and ERA5 SSCs, along with their differences. Both ensembles show a net increase in precipitation over the AIS: 269 Gt for the ERA5-forced CAM ensemble mean and 118 Gt for the ANT-REC-forced CAM ensemble mean (more than twice smaller). As expected, the largest increases are found along coastal regions, where adiabatic cooling during orographic uplift of moist air masses originating from the ocean converts atmospheric humidity into snowfall. A substantial precipitation increase also occurs in non-coastal areas in West Antarctica.
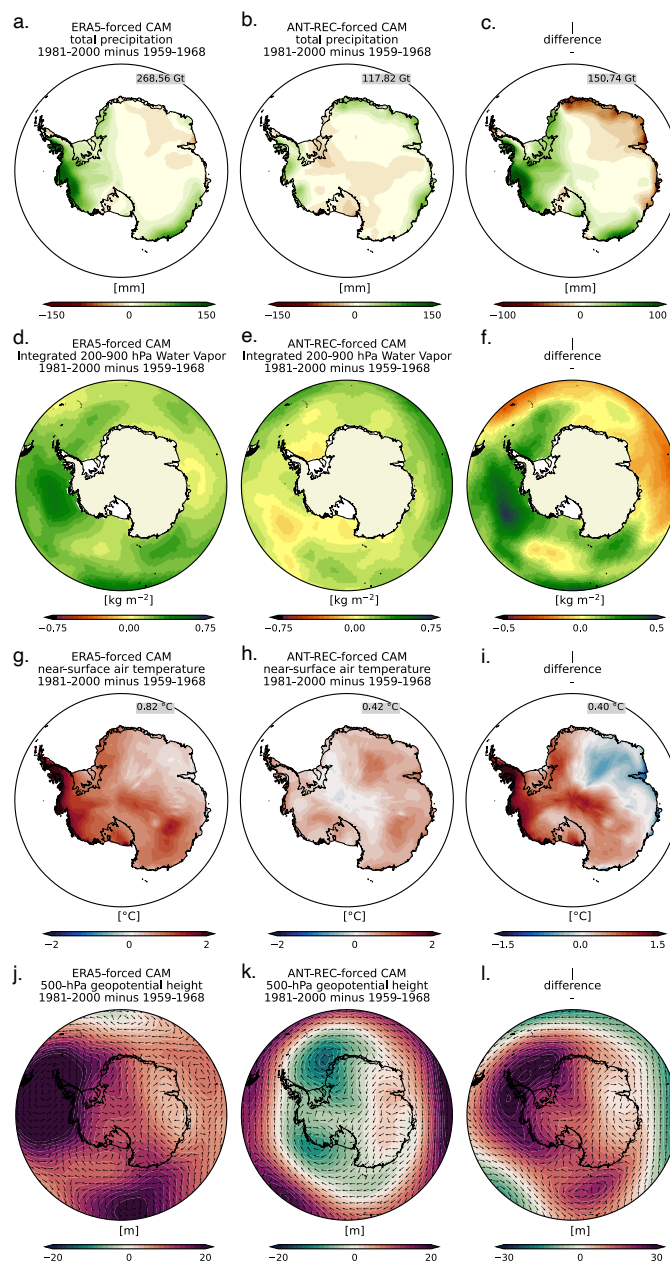
Figure 3. (**a–c**) Total precipitation changes between 1981–2000 and 1959–1968 in ERA5-forced CAM (**a**), ANT-REC-forced CAM (**b**), and their difference (**c**, i.e., **b–a**). (**d–f**) Same as (**a–c**), but for integrated water vapor between 200–900 hPa. (**g–i**) Same, but for near-surface air temperature. (**j–l**) Same, but for 500-hPa geopotential height together with 500-hPa winds (vectors scaled by their norms). For total precipitation and near-surface air temperature, the corresponding continental mean change is also indicated (e.g., precipitation change is computed as the integrated total precipitation for 1981–2000 minus the integrated total precipitation for 1959–1968).

135   The net increase in precipitation in both ensembles is driven by changes in external forcings (aerosols, greenhouse gases, ozone depletion) and by SSC changes. Since external forcings are identical in both CAM ensembles, their differences isolate the impact of SSCs. The ERA5-forced CAM ensemble mean shows a precipitation gain of 151 Gt in 1981–2000 in respect to 1959–1968 relative to the ANT-REC-forced CAM ensemble mean, with the largest positive anomalies in West Antarctica. This enhanced precipitation can be explained by pronounced differences in sea-ice concentration and SSTs in the Bellingshausen

140 and Amundsen Seas (Fig. 1): compared with ANT-REC, ERA5 SSCs show stronger sea-ice retreat and more intense surface ocean warming in this area. These conditions favor enhanced air–sea fluxes, especially upward moisture transfer from the ocean to the atmosphere. Combined with the climatological low-pressure system located off the West Antarctic coasts, known as the Amundsen Sea Low, these changes increase moisture transport toward the West Antarctic Ice Sheet, where it precipitates. In contrast, ANT-REC-forced CAM indicates a strong precipitation increase over Dronning Maud Land, associated with

145 higher offshore atmospheric vapor content and the strengthening of a low-pressure system off the East Antarctic coast in the Altantic/Indian sector, which transports additional moisture inland (Fig. 3). Conversely, ERA5-forced CAM shows anomalous positive changes in 500-hPa geopotential height in this sector, which favors enhanced northward outflow from the cold and dry continent and thus drier conditions compared with ANT-REC-forced CAM.

    For near-surface air temperature, both ensembles simulate overall warming in 1981–2000 relative to 1959–1968: 0.45°C in

150 the ANT-REC-forced CAM ensemble mean and 0.87°C in the ERA5-forced CAM ensemble mean (almost twice as large). Unlike precipitation, warming is not confined to coastal regions but extends across the Antarctic Plateau. Consistent with the precipitation patterns, ERA5-forced CAM shows strong warming over the Antarctic Peninsula and West Antarctica. ANT-REC-forced CAM shows weaker warming in West Antarctica but similarly strong warming over the Antarctic Peninsula (though with lower amplitude) and the Antarctic Plateau. The differences between the two ensembles are thus consistent with those found

155 for precipitation, particularly in West Antarctica and the Antarctic Peninsula. This pattern aligns with the well-documented positive temperature–precipitation relationship over Antarctica (Frieler et al., 2015). However, in East Antarctica, warming is not systematically associated with higher precipitation. For example, in Dronning Maud Land, strong warming in ERA5-forced CAM is not always coincided with notable precipitation changes.

4   Discussion and conclusions

160 According to ERA5, the AIS gained about 440 Gt of surface mass (precipitation) in 1981–2000 relative to 1959–1968 corresponding to 160% and 370% of the increases simulated in the ERA5-forced CAM and ANT-REC-forced CAM ensembles, respectively (Fig. S1). Our model simulations therefore indicate that SSCs in ERA5 cannot, solely, explain the entire precipitation changes in ERA5. For near-surface air temperature, the mean change in ERA5 (0.82 °C) is consistent with ERA5-forced CAM, but the spatial patterns differ: ERA5 shows weaker warming in West Antarctica and stronger warming over the Ross and

165 Filchner–Ronne Ice Shelves. Consequently, precipitation sensitivity to temperature substantially differs between the datasets: 19.8% per °C in ERA5, compared with 12% in ERA5-forced CAM and 10.4% in ANT-REC-forced CAM. The stronger

scaling in ERA5 likely reflects circulation-driven increases in moisture transport rather than a purely thermodynamic Clausius–Clapeyron response.

The largest discrepancies between ERA5 and ERA5-forced CAM are found in the 500-hPa geopotential height field. ERA5
170 shows a strengthening and poleward shift of the westerlies, including intensification of the Amundsen Sea Low, and a pronounced deepening of a low-pressure system near the East Antarctic coast, close to the Amery Ice Shelf. Although this negative trend in the westerly winds is consistent with observations (Fogt et al., 2019), the magnitude is too strong. This exaggerated change is consistent with the positive bias in surface pressure recorded at several East Antarctic stations (Dalaiden et al., 2025), where ERA5 overestimates the negative pressure trend. Associated with this surface atmospheric pressure bias is a cool bias
175 during the pre-satellite period (Fig. 2), also reported by Bromwich et al. (2024). Our modeling experiments suggest that SSCs account for about 30% of this cold bias, but other factors must also contribute.

The aim of this study was to better understand the reported mid-20th century surface mass gain of the AIS, and more generally Antarctic surface climate change, by focusing on the impacts of SSC uncertainties during the pre-satellite era (1958–1978). We show that SSC uncertainties strongly affect the Antarctic hydroclimate, influencing both precipitation and near-
180 surface temperature. In contrast to previous studies, which primarily tested sensitivity using idealized perturbations (e.g., Kittel et al., 2018), we quantify Antarctic climate sensitivity using two observational SSC datasets, thereby providing an explicit quantification of the SSC uncertainty. In particular, simulations using a recent Antarctic reconstruction – assimilating mid- and high-latitude station observations into an Earth System Model (i.e., Dalaiden et al., 2025) – show better agreement with Antarctic observations than simulations using ERA5 SSCs. This suggests that ERA5 SSCs may contain systematic biases
185 in the Southern Ocean. In particular, ERA5 relies on HadISST2 for the period before the satellite period. Yet HadISST2 is characterized by a large sea-ice cover over that period (Titchner and Rayner, 2014). Nonetheless, the better performance of ANT-REC should be interpreted cautiously. By using near-surface air temperature and atmospheric surface pressure from the Antarctic and sub-Antarctic weather stations, this reconstruction relies on the physical relationship between continental and oceanic changes to reconstruct the surface conditions, further used as atmospheric forcing in a ocean–sea-ice model. This
190 later step improves the representation of the variability of the sea surface temperature and sea-ice concentration through the integration of the atmospheric forcing by the ocean (Dalaiden et al., 2025).

Given the critical role of Antarctica in the global climate system, particularly through sea-level rise, longer and more homogeneous SSC records are essential for robust assessments of long-term climate change. This is especially important given the large internal variability of the Antarctic climate (e.g., Jones et al., 2016). Developing a temporally consistent SSC dataset for
195 the high-latitude Southern Hemisphere is therefore a priority. Progress is foreseen by the combination of diverse observational sources – including satellite products, weather stations, historical ship logbooks, as well as indirect climate records – into unified datasets.

Data availability. All datasets used in this study are publicly available from open repositories. Weather station observations were obtained from the READER dataset (https://legacy.bas.ac.uk/met/READER/) and from the University Corporation for Atmospheric Research

200 data archive, dataset ds570.0 (https://rda.ucar.edu/datasets/ds570.0/#!description), along with the Byrd Station temperature record (https://polarmet.osu.edu/datasets/Byrd_recon/). The ERA5 reanalysis was retrieved from the Copernicus Climate Change Service (C3S) Climate Data Store. Sea-ice concentration data from NSIDC are available at https://nsidc.org/data/NSIDC-0051/versions/1. The HadISST2 product can be accessed from https://www.metoffice.gov.uk/hadobs/hadisst2/data/download.html, and the OISST dataset is available from https://www.ncei.noaa.gov/products/optimum-interpolation-sst. The ANT-REC reconstruction is available on Zenodo (https://zenodo.org/records/13828875). Finally, the 10-member ensembles of ERA5-forced CAM and ANT-REC-forced CAM simulations are available on Zenodo (https://zenodo.org/records/17521381).

Author contributions. QD designed the study, performed the simulations with assistance from IB, analyzed the results, and wrote the first draft of the manuscript. IG provided feedback and comments on the initial version of the manuscript.

Competing interests. The authors declare that they have no conflict of interest.

210 *Acknowledgements.* The simulations were performed on the Norwegian supercomputer Betzy (Sigma2; project nn9039k). QD received support from the European Union's Horizon 2020 research and innovation programme under the Marie Skłodowska-Curie grant agreement No. 101149188.

References

Bentsen, M., Bethke, I., Debernard, J. B., Iversen, T., Kirkevåg, A., Seland, Ø., Drange, H., Roelandt, C., Seierstad, I. A., Hoose, C., and
215   Kristjánsson, J. E. (2013). The norwegian earth system model, noresm1-m – part 1: Description and basic evaluation of the physical
       climate. *Geoscientific Model Development*, 6(3):687–720.

Bromwich, D. H., Ensign, A., Wang, S. H., and Zou, X. (2024). Major Artifacts in ERA5 2-m Air Temperature Trends Over Antarctica Prior
       to and During the Modern Satellite Era. *Geophysical Research Letters*, 51(21).

Dalaiden, Q., Goosse, H., Holland, P. R., and Barthelemy, A. (2025). Dynamical reconstruction of Southern Ocean and Antarctic climate
220   variability since 1700. *Scientific data*, 12(1):1574.

Fogt, R. L., Schneider, D. P., Goergens, C. A., Jones, J. M., Clark, L. N., and Garberoglio, M. J. (2019). Seasonal Antarctic pressure variability
       during the twentieth century from spatially complete reconstructions and CAM5 simulations. *Climate Dynamics*, 53(3):1435–1452.

Frieler, K., Clark, P. U., He, F., Buizert, C., Reese, R., Ligtenberg, S. R., Van Den Broeke, M. R., Winkelmann, R., and Levermann, A.
       (2015). Consistent evidence of increasing Antarctic accumulation with warming. *Nature Climate Change*, 5(4):348–352.

225   Fyke, J., Sergienko, O., Löfverström, M., Price, S., and Lenaerts, J. T. (2018). An Overview of Interactions and Feedbacks Between Ice
       Sheets and the Earth System. *Reviews of Geophysics*, 56(2):361–408.

Gates, W. L., Boyle, J. S., Covey, C., Dease, C. G., Doutriaux, C. M., Drach, R. S., Fiorino, M., Gleckler, P. J., Hnilo, J. J., Marlais, S. M.,
       Phillips, T. J., Potter, G. L., Santer, B. D., Sperber, K. R., Taylor, K. E., and Williams, D. N. (1999). An Overview of the Results of the
       Atmospheric Model Intercomparison Project (AMIP I). *Bulletin of the American Meteorological Society*, 80(1):29–55.

230   Good, S., Fiedler, E., Mao, C., Martin, M. J., Maycock, A., Reid, R., Roberts-Jones, J., Searle, T., Waters, J., While, J., and Worsfold,
       M. (2020). The current configuration of the ostia system for operational production of foundation sea surface temperature and ice
       concentration analyses. *Remote Sensing*, 12(4).

Gossart, A., Helsen, S., Lenaerts, J. T. M., Broucke, S. V., van Lipzig, N. P. M., and Souverijns, N. (2019). An Evaluation of Surface
       Climatology in State-of-the-Art Reanalyses over the Antarctic Ice Sheet. *Journal of Climate*, 32(20):6899–6915.

235   Hersbach, H., Bell, B., Berrisford, P., Hirahara, S., Horányi, A., Muñoz-Sabater, J., Nicolas, J., Peubey, C., Radu, R., Schepers, D., Simmons,
       A., Soci, C., Abdalla, S., Abellan, X., Balsamo, G., Bechtold, P., Biavati, G., Bidlot, J., Bonavita, M., De Chiara, G., Dahlgren, P., Dee,
       D., Diamantakis, M., Dragani, R., Flemming, J., Forbes, R., Fuentes, M., Geer, A., Haimberger, L., Healy, S., Hogan, R. J., Hólm, E.,
       Janisková, M., Keeley, S., Laloyaux, P., Lopez, P., Lupu, C., Radnoti, G., de Rosnay, P., Rozum, I., Vamborg, F., Villaume, S., and Thépaut,
       J. N. (2020). The ERA5 global reanalysis. *Quarterly Journal of the Royal Meteorological Society*, 146(730):1999–2049.

240   Hurrell, J. W., Holland, M. M., Gent, P. R., Ghan, S., Kay, J. E., Kushner, P. J., Lamarque, J. F., Large, W. G., Lawrence, D., Lindsay, K.,
       Lipscomb, W. H., Long, M. C., Mahowald, N., Marsh, D. R., Neale, R. B., Rasch, P., Vavrus, S., Vertenstein, M., Bader, D., Collins, W. D.,
       Hack, J. J., Kiehl, J., and Marshall, S. (2013). The community earth system model: A framework for collaborative research. *Bulletin of
       the American Meteorological Society*, 94(9):1339–1360.

Jones, J. M., Gille, S. T., Goosse, H., Abram, N. J., Canziani, P. O., Charman, D. J., Clem, K. R., Crosta, X., De Lavergne, C., Eisenman,
245   I., England, M. H., Fogt, R. L., Frankcombe, L. M., Marshall, G. J., Masson-Delmotte, V., Morrison, A. K., Orsi, A. J., Raphael, M. N.,
       Renwick, J. A., Schneider, D. P., Simpkins, G. R., Steig, E. J., Stenni, B., Swingedouw, D., and Vance, T. R. (2016). Assessing recent
       trends in high-latitude Southern Hemisphere surface climate. *Nature Climate Change*, 6(10):917–926.

Kay, J. E., Deser, C., Phillips, A., Mai, A., Hannay, C., Strand, G., Arblaster, J. M., Bates, S. C., Danabasoglu, G., Edwards, J., Holland, M.,
       Kushner, P., Lamarque, J. F., Lawrence, D., Lindsay, K., Middleton, A., Munoz, E., Neale, R., Oleson, K., Polvani, L., and Vertenstein,

250   M. (2015). The community earth system model (CESM) large ensemble project : A community resource for studying climate change in the presence of internal climate variability. *Bulletin of the American Meteorological Society*, 96(8):1333–1349.

Kittel, C., Amory, C., Agosta, C., Delhasse, A., Doutreloup, S., Huot, P. V., Wyard, C., Fichefet, T., and Fettweis, X. (2018). Sensitivity of the current Antarctic surface mass balance to sea surface conditions using MAR. *Cryosphere*, 12(12):3827–3839.

Lenaerts, J. T., Gettelman, A., van Tricht, K., van Kampenhout, L., and Miller, N. B. (2020). Impact of Cloud Physics on the Greenland Ice
255   Sheet Near-Surface Climate : A Study With the Community Atmosphere Model. *Journal of Geophysical Research Atmospheres*, pages 1–16.

Neale, R., Richter, J., Conley, A., Park, S., Lauritzen, P., Gettelman, A., Williamson, D., Rasch, P., Vavrus, S., Taylor, M., Collins, W., Zhang, M., and Lin, S.-J. (2010). Description of the community atmosphere model (cam 4.0). *NCAR Technical Note*, TN-485+STR.

Otosaka, I. N., Shepherd, A., Ivins, E. R., Schlegel, N.-J., Amory, C., van den Broeke, M. R., Horwath, M., Joughin, I., King, M. D., Krinner,
260   G., Nowicki, S., Payne, A. J., Rignot, E., Scambos, T., Simon, K. M., Smith, B. E., Sørensen, L. S., Velicogna, I., Whitehouse, P. L., A, G., Agosta, C., Ahlstrøm, A. P., Blazquez, A., Colgan, W., Engdahl, M. E., Fettweis, X., Forsberg, R., Gallée, H., Gardner, A., Gilbert, L., Gourmelen, N., Groh, A., Gunter, B. C., Harig, C., Helm, V., Khan, S. A., Kittel, C., Konrad, H., Langen, P. L., Lecavalier, B. S., Liang, C.-C., Loomis, B. D., McMillan, M., Melini, D., Mernild, S. H., Mottram, R., Mouginot, J., Nilsson, J., Noël, B., Pattle, M. E., Peltier, W. R., Pie, N., Roca, M., Sasgen, I., Save, H. V., Seo, K.-W., Scheuchl, B., Schrama, E. J. O., Schröder, L., Simonsen, S. B., Slater, T.,
265   Spada, G., Sutterley, T. C., Vishwakarma, B. D., van Wessem, J. M., Wiese, D., van der Wal, W., and Wouters, B. (2023). Mass balance of the greenland and antarctic ice sheets from 1992 to 2020. *Earth System Science Data*, 15(4):1597–1616.

Titchner, H. A. and Rayner, N. A. (2014). The met office hadley centre sea ice and sea surface temperature data set, version 2: 1. sea ice concentrations. *Journal of Geophysical Research: Atmospheres*, 119(6):2864–2889.

Turner, J. (2004). The El Niño-Southern Oscillation and Antarctica. *International Journal of Climatology*, 24(1):1–31.

270   van Dalum, C. T., van de Berg, W. J., van den Broeke, M. R., and van Tiggelen, M. (2025). The surface mass balance and near-surface climate of the antarctic ice sheet in racmo2.4p1. *EGUsphere*, 2025:1–40.

Wang, W., Shen, Y., Chen, Q., Wang, F., and Yu, Y. (2025). Spatiotemporal mass change rate analysis from 2002 to 2023 over the Antarctic Ice Sheet and four glacier basins in Wilkes-Queen Mary Land. *Science China Earth Sciences*, 68(4):1086–1099.